

Velocities of acoustic streaming in a solid–liquid mixture generated by an ultrasonic wave (Particles and particle concentration)

Junichi OHTA*, Masahiro IGUCHI** and Masahito ONARU**

* Dept. Mechanical Engineering, Graduate School of Engineering, University of Fukui
3-9-1 Bunkyo, Fukui, Fukui 910-8507, Japan
E-mail: ohta@u-fukui.ac.jp

** Dept. Fiber Amenity, Graduate School of Engineering, University of Fukui
3-9-1 Bunkyo, Fukui, Fukui 910-8507, Japan

Received 4 August 2013

Abstract

Progressive ultrasonic waves cause acoustic streaming in a liquid. Although theoretical and experimental studies on acoustic streaming for liquid phase have been carried out, acoustic streaming for a solid–liquid mixture does not seem to have been investigated. The purpose of this study is to clarify the velocity distribution of acoustic streaming in a solid–liquid mixture. An ultrasonic wave with a frequency of 485 kHz was horizontally irradiated on tap water with aluminum particles in a cylindrical tube with a diameter of 120 mm whose orientation was kept horizontal; the acoustic streaming velocities were measured with the irradiation time of the ultrasonic wave, initial particle concentration, and particle shape as the parameters. The following results were obtained: (a) The higher the initial particle concentration is, the faster the acoustic streaming velocity of a solid–liquid mixture becomes; (b) When ultrasonic waves are irradiated on a liquid with heavier solid particles, the acoustic streaming velocity of the solid–liquid mixture decreases with irradiation time to a certain extent.

Key words : Ultrasonic wave, Acoustic streaming, Solid-liquid mixture, Particle, PIV

1. Introduction

Ultrasonic techniques have been put into practice in many applications, e.g., ultrasonic echoes, ultrasonic echo fishfinders, nondestructive testing, ultrasonic flowmeters, ultrasonic cleaning equipment, and ultrasonic motors. However, ultrasonic waves have characteristics that these applications do not take advantage of. When ultrasonic waves are irradiated on particles in a liquid, the particles are aggregated as bands under standing waves. Furthermore, acoustic streaming is known to be generated under progressive ultrasonic waves. According to the scale of the dimensions, acoustic streaming is classified into Schlichting type (inside the boundary layer), Rayleigh type (outside the boundary layer), and Eckart type (straight streaming) (Zarembo,1971)(Kimoto,1985). The case of acoustic streaming outside the boundary layer has been studied theoretically (Rayleigh, 1945). For straight streaming, a calculated velocity profile has been presented inside a closed cylinder under progressive ultrasonic waves Eckart, 1948). Acoustic streaming was widely reviewed and discussed in many cases (Nyborg, 1965).

There have been many reports on the mechanisms of acoustic streaming. Both the non-linearity of fluid-dynamics and the non-linearity of acoustics play important roles in the governing equations of acoustic streaming (Mitome,1998). A driving force of straight streaming, so-called Eckart flow, is reported to be caused by spatial attenuation of a sound pressure amplitude, and to be proportional to the square of the spatial gradient with respect to the envelope of the sound pressure amplitude(Rudenko,1977) (Sato,1994) (Sato, 1997). In a low sound pressure region (at a sound source), acoustic streaming velocity is proportional to the square of sound pressure; in contrast, in a high sound pressure region, the velocity is linearly proportional to the sound pressure(Mitome,1998). A driving force equation of acoustic streaming has been derived for a Gaussian focused beam of an ultrasonic wave(Matsuda,1994) (Kamakura,1995). In a numerical

simulation, the calculated sound pressure and acoustic streaming were reported to be in relatively good agreement with experimental results (Fujii, 1996). A numerical simulation was performed for a liquid with bubbles in a rectangular duct under irradiation of ultrasonic waves from one end, demonstrating time-averaged acoustic streaming of Rayleigh type (Ruggles, 2005).

As mentioned above, particles in a liquid are known to be aggregated as bands under ultrasonic standing waves; however, one of the authors revealed that particles in water under ultrasonic waves generated by a circular-plate acoustic transducer can be aggregated as a band, point, particle clump, or non-aggregation, depending on the experimental conditions (Ohta, 2005) (Ohta, 2007), (Ohta, 2008). Acoustic streaming generated by progressive waves can take particles away from a solid–liquid mixture. Hence, acoustic streaming can be expected to be useful for particle removal, particle transportation, and mixing of a liquid in a vessel by irradiating ultrasonic waves from outside the vessel, without the need for a pump or a stirrer inside the vessel.

To realize the abovementioned applications of acoustic streaming in practice, it is desirable to obtain the relationship between acoustic streaming and particle concentration, properties of the turbulence produced by acoustic streaming, and the effects of particle properties and acoustic frequency on acoustic streaming. Moreover, a calculation of acoustic streaming is expected for a solid–liquid mixture. Although there have been studies on experimental and theoretical acoustic streaming for a single-phase medium, little is yet known about acoustic streaming of a solid–liquid mixture. The purpose of the present study is to clarify the velocity distribution of acoustic streaming in a solid–liquid mixture.

As basic research on acoustic streaming of a solid–liquid mixture, velocities of acoustic streaming (Eckart type) are measured by particle image velocimetry (PIV) (VSJ, 2002), using the particle concentration, irradiation time, and shape of particle as the parameters, in order to clarify the effects of these parameters on the acoustic streaming.

2. Nomenclature

C_0	: Initial particle concentration	
d	: diameter of particle	μm
f	: Frequency of ultrasonic wave	kHz
X	: Distance normal to the Z direction in a horizontal plane	m
Z	: Axial distance from coordinate origin (irradiation direction)	m
z	: Characteristic acoustic impedance	Ns/m^3
ρ	: Density of particles	kg/m^3

3. Experimental Apparatus and Method

3.1. Experimental apparatus

An experimental apparatus and the layout for flow visualization are shown in Fig. 1 and Fig. 2, respectively. The apparatus consists of a cylindrical vessel, a rectangular vessel, a disk-type acoustic transducer, a matching box, a power amplifier, a function generator, and an absorber. The cylindrical vessel is constructed of transparent acrylic resin ($z = 3.3 \times 10^6 \text{Ns/m}^3$) and has an inner diameter of 120 mm and axial length of 250 mm. The disk-type acoustic transducer (diameter: 50 mm) is installed at one end (left-hand side in Figs. 1 and 2) of the cylindrical vessel, and the absorber (diameter: 110 mm) is installed at the other end (right-hand side). The absorber consists of many wedge-shaped rubber pieces attached to each other. Most of the cylindrical vessel is submerged in a rectangular vessel to avoid refraction of light; only a small part of the upper wall of the cylindrical vessel is open to the atmosphere. An electric signal supplied by the function generator is amplified by the power amplifier and then sent to the acoustic transducer, which horizontally irradiates ultrasonic waves. A frequency of 485 kHz was chosen for the ultrasonic waves. The center of the acoustic transducer surface is taken as the origin of coordinates. The normal direction to the transducer surface is defined as the Z (horizontal) direction, and the vertical direction is defined as the Y direction. The direction perpendicular to the Z and Y axes is defined as the X direction. For flow visualization, a laser light sheet was created by a continuous-wave Ar-ion laser and a cylindrical lens.

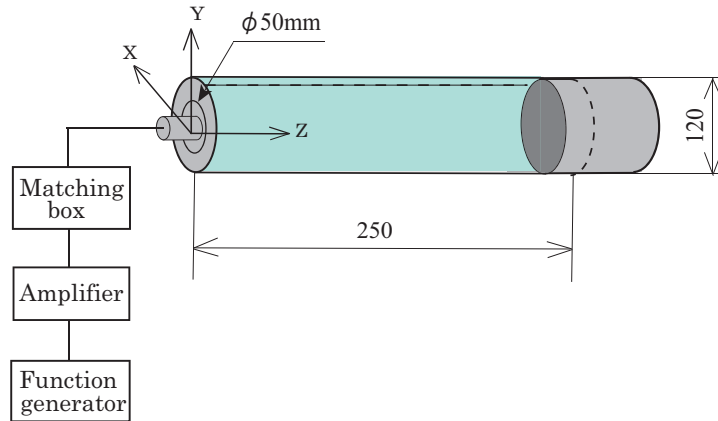


Fig. 1 Schematic diagram of experimental apparatus

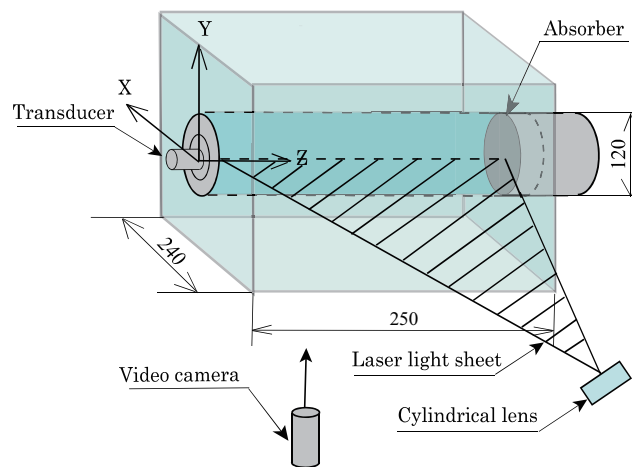


Fig. 2 Experimental apparatus of velocity measurement

3.2. Particles

Nylon 12, aluminum particles (Al-particles), and aluminum flakes were used as solid particles in a liquid as follows:

- (1) Nylon 12 (spherical): average diameter $d = 52.8 \mu\text{m}$ with a standard deviation of $3.7 \mu\text{m}$, acoustic impedance $z = 2.7 \times 10^6 \text{Ns/m}^3$, density $\rho = 1020 \text{kg/m}^3$, (Trial Co., Ltd., Japan).
- (2) Al-particles (spherical): diameter $d = 6.3 \mu\text{m}$ with a standard deviation of $3.0 \mu\text{m}$, acoustic impedance $z = 1.7 \times 10^7 \text{Ns/m}^3$, density $\rho = 2698 \text{kg/m}^3$, (Toyo Aluminum K.K, Japan).
- (3) Aluminum flakes (non-spherical): thin flattened pieces. For two dimensional measurements, an average size of aluminum flakes is $13.7 \mu\text{m}$ with a standard deviation of $5.4 \mu\text{m}$, and the maximum and minimum sizes are $31.3 \mu\text{m}$ and $2.9 \mu\text{m}$. acoustic impedance $z = 1.7 \times 10^7 \text{Ns/m}^3$, density $\rho = 2698 \text{kg/m}^3$, (Wako Pure Chemical Industries, Ltd., Japan). A photo of an aluminum flake taken by SEM is shown in Fig. 3. The minimum scale value is $5 \mu\text{m}$ in the lower part of Fig. 3.

Al-particles are chosen since pure particles of different shapes (spherical and flake) are commercially available, spherical Al-particles of suitably small size are available, and the acoustic impedance of aluminum is sufficiently different from that of water.

3.3. Experimental method

Tap water ($z = 1.5 \times 10^6 \text{Ns/m}^3$) passed through a filter was used to fill the cylindrical vessel. Bubbles in the vessel were removed and the water temperature was adjusted so that initial water temperature was 16.4 to $17.3 \text{ }^\circ\text{C}$ (around $17 \text{ }^\circ\text{C}$). Temperature rise during experiments was kept to less than $0.5 \text{ }^\circ\text{C}$ due to the water in the surrounding rectangular vessel and the surrounding cold air. Dissolved oxygen levels of the tap water were measured with a dissolved oxygen measurement device and were 7.5 to 7.9 mg/l . A predetermined amount of particles was mixed into the tap water. After movement of the water stabilized, ultrasonic waves at a frequency of 485 kHz were horizontally irradiated on the mixture

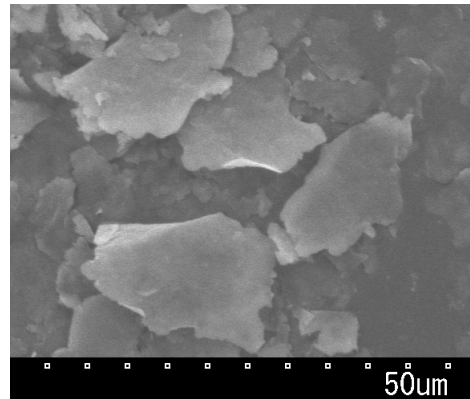


Fig. 3 Photo of aluminum flakes

of the particles and water. The two-dimensional $X - Z$ plane through the irradiation central axis was illuminated with the laser light sheet as shown in Fig. 2. The visualized region of the $X - Z$ plane was recorded with a digital video camera at a shutter speed of $1/250$ s and a frame rate of 30 FPS. The obtained video was transferred to a personal computer and a series of consecutive video frames was extracted as a sequence of still images. The background was eliminated from the original still images, and then PIV was applied to obtain velocity vectors. An average velocity vector at each grid point was obtained from velocity vectors over 33 seconds (990 frames). The parameters in PIV were decided according to a PIV handbook (VSJ, 2002). Before the experiments, a transparent scale was placed along the Z direction in the water of the cylindrical vessel and recorded under the same conditions as those of the velocity measurement. The scale image was used for calibration. The authors regarded irradiation time and volumetric particle concentration as the important parameters.

The irradiation time is defined as the elapsed time from irradiation start. In the present study, the volumetric particle concentration, that is, (mass of particles/particle density) / (volume of the mixture of particle and water), was defined as the particle concentration. The mass of particles was chosen so as to match a predetermined volumetric concentration and measured with an electric balance. A mixture of the Al-particles and a small amount of water was left to sit for more than 24 hours to allow the particles to become wet, and then the mixture was added to the water inside the cylindrical vessel to obtain the predetermined particle concentration of a solid-liquid mixture. When gas remains attached to the particles, the acoustic streaming velocity becomes more than five times higher. Therefore, we first confirmed that no such abnormal velocity could be observed before conducting velocity measurements.

4. Results and Discussions

4.1. Experiment for nylon particle

The spherical nylon particles were used as tracers in velocity measurement for a single medium (tap water). Since the acoustic impedance of the nylon particles is similar to that of water, a mixture of water and nylon particles behaves like a single-phase medium. A velocity profile began to develop from the start of the ultrasonic wave irradiation. According to naked-eye observation, there existed large circulations, i.e., tap water near the acoustic transducer on the central axis moved to the absorber, impinging the absorber, and flowed back to the acoustic transducer along the side wall of the cylindrical vessel. This flow corresponds to the Eckart flow in a closed cylindrical vessel.

In Fig. 4, measured average axial velocities (nylon particle velocities) are plotted against Z on the irradiation axis ($X = Y = 0$ mm) for irradiation times of 5, 10, and 15 minutes (■, ●, and ▲, respectively) for parameters set at an initial particle concentration of $9.8 \times 10^{-5}\%$, a frequency of $f = 485$ kHz, and an output power of $N = 4$ W. In the figure, bars indicating the 95% uncertainty range (ASME, 1985) at the corresponding three measurement times are also shown. From Fig. 4, it is seen that the axial acoustic streaming velocities in the Z direction are low and are not much affected by the irradiation time.

4.2. Particle velocity

4.2.1. Initial aluminum particle concentration The effect of the initial concentration of Al-particles was examined. An example of axial Al-particle velocities including bars indicating the 95% uncertainty range is shown along the irradiation axis (Z direction) for $f = 485$ kHz at $N = 4$ W in water and an irradiation time of 10 minutes at initial particle

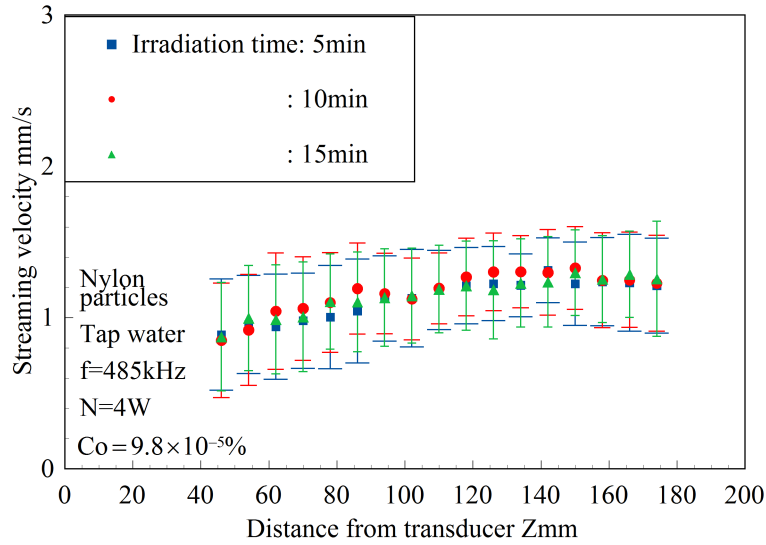


Fig. 4 Streaming velocity in a single phase

concentrations of $3.3 \times 10^{-5}\%$, $4.9 \times 10^{-5}\%$, and $9.8 \times 10^{-5}\%$ (■, ●, and ▲, respectively) in Fig. 5. From this figure it is clear that the higher the particle concentration becomes, the faster the Al-particles move. As Z increases, the axial velocity of aluminum in the Z direction increases, but the velocity gradient with respect Z decreases. Comparing Fig. 5 with Fig. 4, it can be clearly seen that the Al-particle velocity is higher than the single-phase acoustic streaming velocity (nylon velocity).

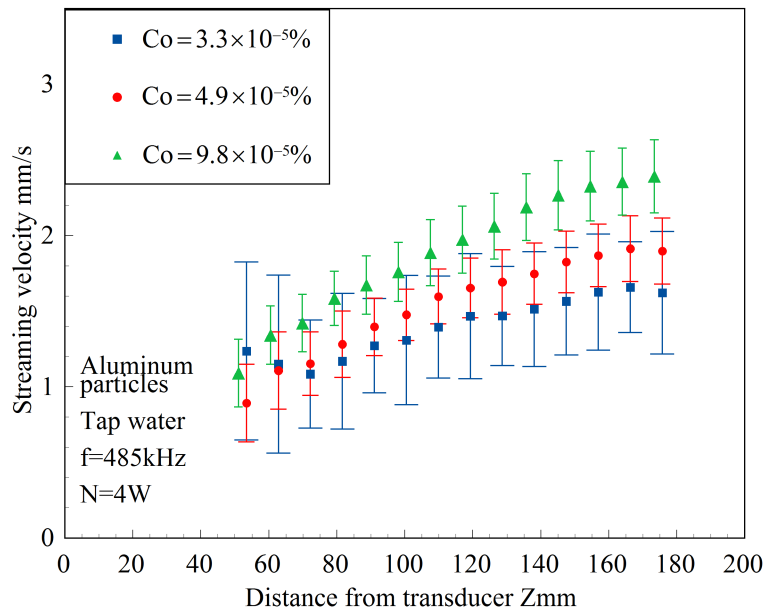


Fig. 5 Effect of initial particle concentration on streaming velocity (aluminum particles)

The relationship between particle concentration and particle velocity is next considered. Firstly, we propose a working hypothesis that acoustic forces on particles (King, 1934) (Yosioka and Kawasima, 1955) (Doinikov, 1994) dominate the movement of the particles under progressive waves. If this working hypothesis is true, then the particles should flow with a large slip velocity between the water and the Al-particles. Under much lower concentrations of solid-liquid mixture, even if the Al-particle concentration increases, the acoustic force on each particle should not change and each Al-particle should not move faster. Since the velocity of Al-particles becomes high with increasing particle concentrations, as shown in Fig. 5, the current working hypothesis cannot explain the observations.

Next, we propose a new working hypothesis that the slip velocity between an Al-particle and water is negligibly small and the mixture of Al-particles and water flows together with almost the same velocity. If the particle concentration

increases, then ultrasonic waves should attenuate through the mixture in the Z direction (the irradiation direction), and a time-averaged sound pressure gradient with respect to Z , i.e., dp/dZ , the negative gradient, should increase. Hence, the force acting on a control volume of the mixture in the Z direction should increase with increasing initial particle concentration, so that the axial velocity of the mixture should also increase. This explanation is similar to that a sound pressure gradient with respect to the irradiation axis, i.e., spatial attenuation, causes acoustic streaming for a single medium. Since the estimated Stokes number for the Al-particles in the mixture under the conditions of the case shown in Fig. 5 is approximately zero, i.e., 10 to the minus fifth power, the particles have ample time to respond to changes in liquid velocity. Therefore, the greater the Al-particle concentration becomes, the faster the Al-particles should flow. The experimental results of Fig. 5 support this latter hypothesis. Moreover, the velocities of the Al-particles are higher than those of the single-phase medium. The reason inferred is that the former have a larger time-averaged pressure attenuation in the Z direction than the latter because of scattering of ultrasonic waves.

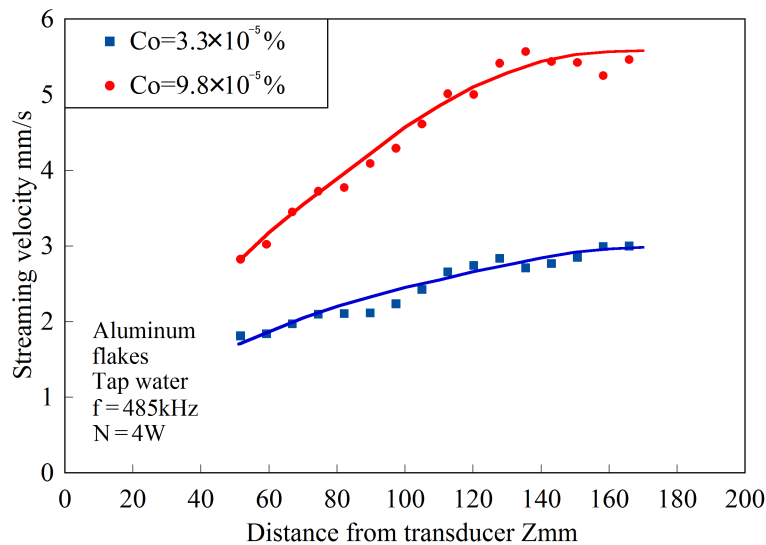


Fig. 6 Effect of initial particle concentration on streaming velocity (aluminum flakes)

4.2.2. Initial aluminum flake concentration Measured axial velocities of aluminum flakes on the irradiation axis are shown after 10 minutes of irradiation at initial particle concentrations of $3.3 \times 10^{-5} \%$ and $9.8 \times 10^{-5} \%$ in Fig. 6. The measured velocity for $9.8 \times 10^{-5} \%$ is higher than that of $3.3 \times 10^{-5} \%$. This demonstrates, therefore, that the greater the concentration is, the faster the aluminum flakes move. The axial velocity gradient with respect to Z decreases along the irradiation axis, especially near the absorber. The velocity gradient was reported to decrease near the boundary of the downstream side for a single-phase upward acoustic streaming (Fujii 1996). Hence, the change in the velocity gradient is attributed to the effect of the downstream end of the cylinder. When the initial concentration of aluminum flakes increased even further, wavy flows with relatively large eddies (smaller than the recirculation eddy of the entire cylinder) were observable to the naked eyes. The aluminum flake size ranges. In such high particle concentrations the aluminum flakes are located very closely and particle clusters may be easily formed. Thus, there is possibility to cause non-symmetrical acoustic radiation forces or drag forces with respect to the irradiation axis. This non-symmetrical forces may trigger the wavy flow.

4.3. Irradiation time of ultrasonic waves

An Al-particle velocity profile began to develop immediately at the start of ultrasonic wave irradiation, and fully developed in several minutes. Experiments were carried out to examine the effect of irradiation time on axial velocity profiles. Averaged measured axial velocities of Al-particles with bars indicating the 95% uncertainty range are plotted against the Z direction on the irradiation axis for an initial particle concentration of $9.8 \times 10^{-5} \%$, $f = 485$ kHz at $N = 4$ W in tap water, with the irradiation time as the parameter in Fig. 7. Al-particle velocities are shown at irradiation times of 5, 10, and 15 minutes (■, ●, and ▲, respectively) along with nylon particle velocity (single-phase flow: ◆) in Fig. 7. As shown, the Al-particle velocities decrease as irradiation time increases. One possible explanation for this phenomenon is degassing of the tap water due to the continuous ultrasonic wave irradiation. However, this is not true in this case because the acoustic streaming velocity profile of tap water (single-phase medium) did not change over 10 to 60 minutes

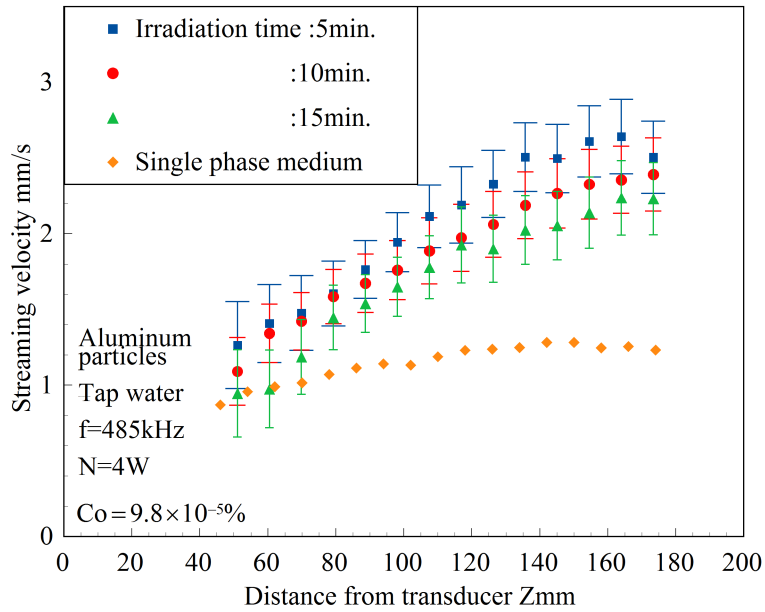


Fig. 7 Effect of irradiation time on streaming velocity (aluminum particles)

of continuous ultrasonic wave irradiation in other experiments carried out by the the authors. To consider this matter further, simultaneously flowing Al-particles and tap water at irradiation times of 5, 10, and 15 minutes are shown in the range of $z = 80\text{--}140\text{ mm}$ in Figs. 8(a), (b), and (c). From these pictures, since the density of Al-particles is greater than that of water, some Al-particles sink, and the particle concentration decreases with irradiation time due to gravity. Therefore, the reduction of the Al-particle velocity with irradiation time is attributed to the decrease in the particle concentration, as was discussed in section 4.2.1. The nylon particle velocity profiles (representing water velocity) shown in Fig. 4 remain unchanged for 15 minutes because the density of nylon particles is approximately equal to that of water. As the irradiation time increases, the velocity profiles for Al-particles will approach that of a single-phase medium (water).

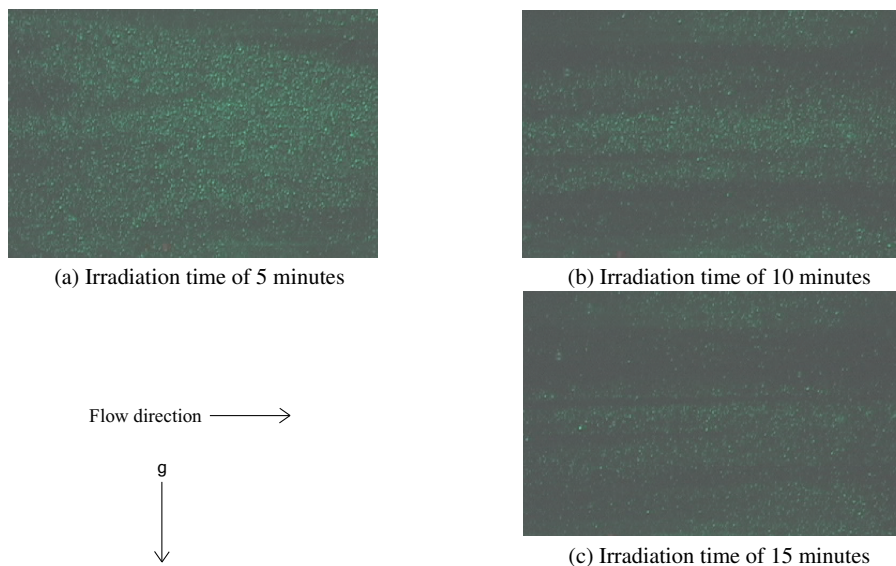


Fig. 8 Variation of particle concentration with irradiation time (aluminum particles, $f = 485\text{ kHz}$)

4.4. Aluminum flakes and aluminum particles

Here we consider the effect of particle shape on acoustic velocity. Aluminum flakes were chosen to represent particles having a non-spherical shape. Example of Al-particles (spherical), aluminum flakes, and nylon particles (spherical) axial

velocities, shown as ■, ●, and ▲, respectively, are plotted against Z for an initial particle concentration of $9.8 \times 10^{-5}\%$, $f = 485 \text{ kHz}$ in tap water, and the irradiation time of 10 minutes in Fig. 9. Comparing Al-particles with aluminum flakes, it is seen that the latter move faster than the former (spherical). We discuss effects of the particle number density, particle size, and particle shape on the difference in velocity. An average particle size of the aluminum flakes is greater than that of the aluminum particles and those volumetric concentrations are same, so it is deduced that the particle number density for the aluminum flakes is lower than that for the aluminum particles. As is seen in Subsections 4.2.1 and 4.2.2, the higher the particle concentration is, the faster the particles move. Thus, from the view point of particle number density, the aluminum flakes should move slower. Figure 9, however, shows that the aluminum flakes move faster. Thus, the particle number density can not explain the velocity difference. Next, as to a particle size, a larger acoustic radiation force acts on a larger object under the same acoustic condition (King,1934)(King, 1935). Hence, one reason of the difference in velocity is attributed to the particle size. Finally, according to our observations, aluminum flakes, whose shapes are similar to small flat plates, seemed to shine brighter and darker repeatedly. From the observations we infer that the aluminum flakes moved with changing their orientation. Hence, ultrasonic waves are likely to be more scattered in the mixture of aluminum flakes–water. The time–averaged axial sound pressure gradient with respect to Z may increases. Thus, there is possibility that the particle shape and their behavior affect the velocity.

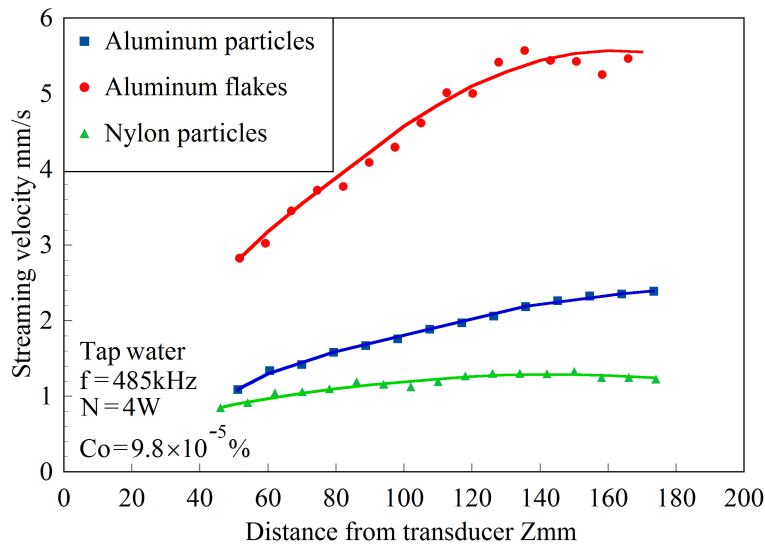


Fig. 9 Effect of particle shape on streaming velocity

5. Conclusions

Ultrasonic waves were horizontally irradiated and the acoustic streaming of a solid–liquid mixture was studied in a closed horizontal cylinder. Experiments were carried out using the irradiation time, particle concentration, particle material, and particle shape as the parameters. The following results were obtained for the conditions of the present experiment:

(1) For acoustic streaming of a single-phase medium (liquid), the velocity profile began to develop from the start of the ultrasonic wave irradiation and the developed velocity profile did not change for the period from 5 to 15 minutes after start.

(2) The acoustic streaming velocity of a solid–liquid mixture was faster than that of a single-phase medium (liquid).

(3) The greater the initial particle concentration of the solid–liquid mixture was, the faster the mixture flowed.

(4) Acoustic streaming velocity decreased for a mixture of a liquid and heavier particles in low particle concentrations as the particle concentration decreased with the irradiation time due to gravity.

(5) Acoustic streaming velocity for the present aluminum flakes was higher than that for the spherical aluminum particles.

6. Acknowledgements

Part of this study was supported by the Japan Society for the Promotion of Science under the Grant-in-Aid-for Scientific Research (C) project No. 20560151. The authors wish to express their thanks to Prof. T. Honda at the University of Fukui for taking a picture of the particles, Mr. M. Atsumi, Mr. Y. Hatayama, and Mr. H. Nakano, former graduate students, and Y. Ohinish, a former undergraduate student, for improving the experimental method and the PIV measurement technique. An acknowledgement is also extended to Toyo Aluminum K. K. (Japan) for supplying the aluminum particles.

References

- ANSI/ASME, ASME performance test code, supplement on instruments and apparatus, Part 1 Measurement Uncertainty, PTC.19.1, (1985), Translated by JSME, Measurement Uncertainty, (1987) (in Japanese).
- Clift, R., Grace, J. R., Weber, M. E., Bubbles, drops, and particle, Academic Press Inc. (1978) pp.111-111.
- Doinikov, A. A., Acoustic radiation pressure on a rigid sphere in a viscous liquid, Proc. R. Soc. Lond. A, Vol. 447, (1994), pp. 447-466.
- Eckart, C., Vortices and streams caused by sound waves, Physical Review, Vol. 73, No. 1 (1948), pp. 68-76.
- Fujii, M., Izumi, Y., Zhang, X., Numerical analysis and measurement of acoustic streaming, Trans. of Acoustic Society of Japan (Nihon Onkyogakkaishi), Vol. 52, No. 5 (1996), pp. 327-332 (in Japanese).
- Kamakura, T., Matsuda, K., Kumamoto, Y., Breazeale, M. A., Acoustic streaming induced in focused gaussian beams, J. Acoustic Society of America, Vol. 97, No. 5, Pt. 1 (1995), pp. 2740-2746.
- Kimoto, H., Acoustic streaming and heat transfer, Gekkan Fijikkusu, Vol. 6, No. 3, (1985), pp.187-191 (in Japanese).
- King, L. V., On the acoustic radiation pressure on spheres, Proc. Royal Soc. A, Vol. 147 (1934), pp. 212-240.
- King, L. V., On the acoustic radiation pressure on circular discs: inertia and diffraction corrections, Proc. Royal Soc. A, Vol. 153 (1935), pp. 1-16.
- Matsuda, K., Kamakura, T., Kumamoto, Y., Theoretical study on acoustic streaming generated in a focused Gaussian beam, Trans. of Acoustic Society of Japan (Nihon Onkyogakkaishi), Vol. 50, No. 12 (1994), pp. 997-1005 (in Japanese).
- Mitome, H., The mechanism of generation of acoustic streaming, Electronics and Communications in Japan, Part 3, Vol. 81, No. 10, (1998), pp. 1-8.
- Nyborg, W. L., Chap. 11 Acoustic streaming, Physical Acoustics, Vol. II, Pt. B, W.P. Mason, Ed. (Academic Press, New York) (1965), pp. 265-331.
- Ohta J., Makara, T., Hirobe, S., Effects of ultrasound on behavior of fine solid particles in solid-liquid mixture (first report, horizontal irradiation in stationary solid-liquid mixture), Trans. JSME B, Vol. 71, No. 701 (2005), pp. 126-132 (in Japanese).
- Ohta, J., Makara, T., Hirobe, S., Effects of ultrasound on behavior of fine solid particles in a solid-liquid mixture (horizontal irradiation in a stationary solid-liquid mixture), J. Fluid Science and Technology, Vol. 2, No. 1 (2007), pp. 77-87.
- Ohta, J. and Nakano, H., Effects of ultrasound on behavior of fine solid particles in solid-liquid mixture (classification of particle aggregation and sound pressure profiles under horizontal irradiation), J. Fluid Science and Technology, Vol. 3, No. 5 (2008), pp. 656-665.
- Rayleigh, J. W. S, The theory of sound, 352, Dover Publication (1945), pp.33-37.
- Rudenko, O.V.and Soluyan, S. I., Theoretical foundations of nonlinear acoustics, Consultants Bureau New York (1977), pp. 187-211.
- Ruggles, A. E., Numerical simulation of acoustic streaming in gas-liquid two-phase flow, Proc. of ASME 2005 Fluids Engineering Division Summer Meeting (FEDSM2005) Paper No. FEDSM 2005-77305, (2005), pp. 893-898.
- Sato, M. and Sugai, H., Analysis of acoustic streaming and its application for mixing in a high pressure vessel, Technical Report of IEICE, US94-61 (1994), pp. 1-8 (in Japanese).
- Sato, M., Sugai, H., Fujii, T., Mechanism of an acoustic streaming by absorption of phonon, Transaction of Acoustic Society of Japan (Nihon Onkyogakkaishi), Vol. 53, No. 5 (1997), pp. 352-355 (in Japanese).
- The Visualization Society of Japan, Handbook of PIV, Morikita Publishing Co. Ltd., (2002) (in Japanese).
- Yosioka, K. and Kawasima, Y., Acoustic radiation pressure on a compressible sphere, Acustica, Vol. 5 (1955), pp. 167-173.

Zarembo, L.K., Acoustic streaming, High-Intensity Ultrasonic Fields, edited by L. D. Rozenberg (Plenum, New York,), Vol. 85, (1971), pp. 137-199.